Acta Mechanica Sinica (2012) 28(4):1106–1114
DOI 10.1007/s10409-012-0091-x

RESEARCH PAPER

Large conversion of energy in dielectric elastomers by electromechanical phase transition

Tong-Qing Lu · Zhi-Gang Suo

Received: 9 April 2012 / Revised: 26 June 2012 / Accepted: 26 June 2012

Abstract When air is pumped in, a tubular balloon initially inflates slightly and homogeneously. A short section of the balloon then forms a bulge, which coexists with the unbulged section of the balloon. As more air is pumped in, the bulged section elongates at the expense of the unbulged section, until the entire balloon is bulged. The phenomenon is analogous to the liquid-to-vapor phase transition. Here we study the bulging transition in a dielectric elastomer tube as air is pumped into the balloon and a voltage is applied through the thickness of the membrane. We formulate the condition for coexistent budged and unbulged sections, and identify allowable states set by electrical breakdown and mechanical rupture. We find that the bulging transition dramatically amplifies electromechanical energy conversion. Energy converted in an electromechanical cycle consisting of unbulged and bulged states is thousands of times that in an electromechanical cycle consisting of only unbulged states.

Keywords Dielectric elastomer · Bulge · Electromechanical energy conversion · Tubular balloon · Electromechanical transition

1 Introduction

The recent decade has seen the emergence of dielectric elastomers as materials of choice for the artificial-muscle technology [1]. Attributes include large deformation, fast response, light weight, silent operation, low maintenance, and low cost [2–4]. The deformation of dielectric elastomers can be induced by applying either a voltage or a force. The voltage-induced deformation is exploited in actuators in soft robots [5, 6], adaptive optics [7], bioengineering [8] and programmable haptics [9]. The force-induced deformation changes the capacitance of the elastomers, and is exploited in generators for harvesting energy from human movements and ocean waves [10–12].

The performance of a transducer is markedly affected by how it is loaded. Consider a transducer made of a membrane of a dielectric elastomer sandwiched between two compliant electrodes (Fig. 1). When the electrodes are subject to a voltage, the positive and negative charges spread on the two faces of the membrane, causing the membrane to reduce its thickness and expand its area. The capacitance of the membrane is proportional to its area and is inversely proportional to its thickness. Recall that elastomers are typically incompressible, so that the capacitance of the membrane is quadratic in its area. If the membrane is subject to equal-biaxial stretches, the capacitance scales with the stretch to the fourth power. For example, a commonly used acrylic elastomer, VHB, is readily stretched six times equal-biaxially; such a deformation increases the capacitance by a factor of $6^4 = 1\,296$. However, if the membrane is clamped in one direction and stretched in the other direction (i.e., stretched under the pure-shear condition), the capacitance is quadratic in the stretch. If the membrane is stretched by a uniaxial force, the capacitance is linear in the stretch.

The loading conditions also markedly affect the electromechanical instability, also known as the pull-in instability [13]. As the thickness decreases, the electric field increases. If this positive feedback prevails over the strain-stiffening of the elastomer, the membrane becomes unstable and thins down dramatically. The pull-in instability often leads to electrical breakdown, and has been considered as a mode of failure [14–17]. A suitably designed

T.-Q. Lu
State Key Lab for Strength and Vibration of Mechanical Structures,
International Center of Applied Mechanics,
School of Aerospace Engineering,
Xi'an Jiaotong University, 710049 Xi'an, China

T.-Q. Lu · Z. G. Suo (✉)
School of Engineering and Applied Sciences,
Harvard University, Cambridge,
MA 02138, USA
email: suo@seas.harvard.edu

transducer, however, can operate on the verge of the pull-in instability without electrical breakdown, leading to giant voltage-induced deformation [18, 19]. An acrylic elastomer has been shown to achieve voltage-induced expansion in area by 158% with a membrane biaxially prestretched and fixed to a rigid frame [20] by 260% with a membrane constrained by two rigid clamps [21] by 488% with a membrane subject to biaxial dead loads [22] and by 1 689% with a membrane mounted on a chamber of compressed air [23].

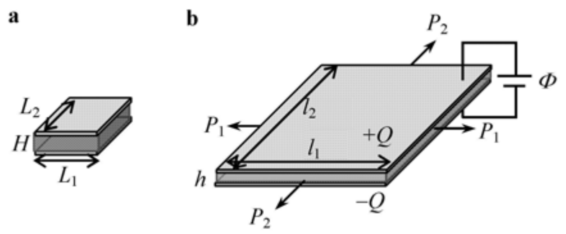

Fig. 1 In the reference state, an undeformed and uncharged membrane of a dielectric elastomer is sandwiched between two compliant electrodes. In an actuated state, the membrane is subject to forces in the plane and a voltage through the thickness. **a** Reference state; **b** Actuated state

The pull-in instability can also lead to an electromechanical phase transition. For example, a pre-stretched membrane under a voltage can deform into coexistent regions of two types, one being flat and the other wrinkled [24]. This experimental observation has been interpreted theoretically as follows [25, 26]. The membrane is thick in the flat regions, and thin in the wrinkled regions. At a certain voltage, localized regions of the membrane undergo the pull-in instability and become thin. The pull-in instability, however, does not cause electrical breakdown. Rather, the thickness of the thin regions is stabilized by the steep strain-stiffening of the elastomer, so that the thin regions survive the pull-in instability without electrical breakdown, and coexist with the thick regions. Because the volume of the elastomer is incompressible, the thin regions must expand in area. This expansion is constrained by the surrounding thick regions, causing the thin regions to form wrinkles. As more charge is supplied to the membrane, the thin regions enlarge at the expense of the thick regions, until the entire membrane becomes thin. The phenomenon is analogous to the liquid-to-vapor phase transition.

It is tempting to push this analogy further. A steam engine or a refrigerator operates by cycling a working fluid through the liquid-vapor phase transition. The transition is accompanied with large changes in entropy and volume, enabling robust thermomechanical energy conversion [27]. By analogy, the transition from a thick membrane to a thin membrane is accompanied with large changes in charge and area, enabling robust electromechanical energy conversion. In a previous analysis of dielectric elastomers under uniaxial forces, however, the electromechanical phase transition was predicted to occur at an electric field above the electrical breakdown strength of existing dielectric elastomers [28].

Here we propose a setup in which an electromechanical phase transition occurs far more readily. The setup involves a common experience with a tubular balloon (Fig. 2). When air is pumped in, the balloon initially inflates slightly and homogeneously. A short section of the balloon then forms a bulge, which is in equilibrium with the unbulged section of the balloon. As more air is pumped in, the bulged section elongates at the expense of the unbulged section, until the entire balloon is bulged. The propagating bulges have been used daily by balloon artists [29] and analyzed occasionally by scientists [30–32]. Here we study the bulging transition induced by simultaneously pumping air into the tube and applying a voltage through the thickness of the membrane. We formulate the condition for coexistent budged and unbulged sections. We regard a balloon as a thermodynamic system of two degrees of freedom, and represent the states of the balloon on two dimensional diagrams, such as the voltage-stretch diagram, voltage-charge diagram, and pressure-volume diagram. In such a diagram, we identify the region of allowable states by plotting conditions of failure, such as electrical breakdown and mechanical rupture. We find that the bulging transition dramatically amplifies electromechanical energy conversion. Energy converted in an electromechanical cycle consisting of unbulged and bulged states is thousands of times that in an electromechanical cycle consisting of only unbulged states.

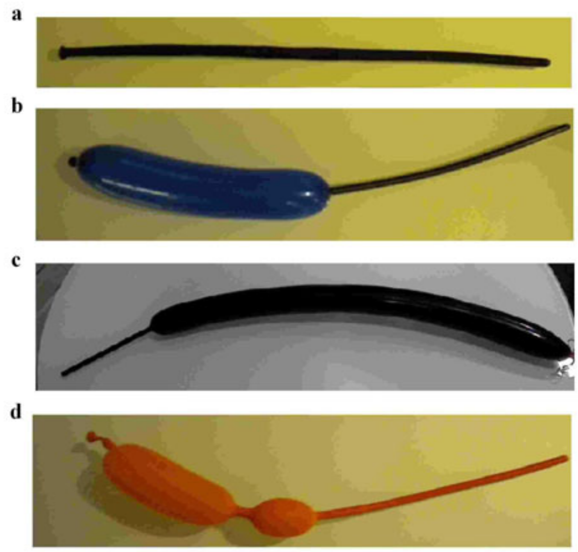

Fig. 2 When air is pumped into a tubular balloon, a small section of the balloon forms a bulge, which coexists with the unbulged section. As more air is pumped in, the bulged section elongates at the expense of the unbulged section, until the entire balloon is bulged. One can also squeeze the balloon to arrange multiple bulges to coexist with the unbulged section. **a** Before pumping; **b** After pumping; **c** Pumping with more air; **d** Multiple states

2 Model of ideal dielectric elastomers

The theory of dielectric elastomers has been reviewed recently [33]. Here we summarize the key ideas relevant to this work (Fig. 1). In the reference state, subject to no force and no voltage, a membrane of a dielectric elastomer is of thickness H and lengths L_1 and L_2. The membrane is sandwiched between two compliant electrodes. In an actuated state, subject to forces P_1 and P_2 in the plane and voltage Φ through the thickness, the membrane is of thickness h and lengths l_1 and l_2, while charges $+Q$ and $-Q$ are spread over the two electrodes. Define the stresses as $\sigma_1 = P_1/(l_2 h)$ and $\sigma_2 = P_2/(l_1 h)$, the stretches as $\lambda_1 = l_1/L_1$ and $\lambda_2 = l_2/L_2$, the electric field as $E = \Phi/h$, and the electric displacement as $D = Q/(l_1 l_2)$.

We adopt the model of ideal dielectric elastomers. This model assumes that the membrane is incompressible ($hl_1l_2 = HL_1L_2$), and that the elastomer is a linear dielectric

$$D = \varepsilon E, \tag{1}$$

with the permittivity ε being a constant independent of deformation. The stress-stretch relations are

$$\sigma_1 + \varepsilon E^2 = \lambda_1 \frac{\partial W_s(\lambda_1, \lambda_2)}{\partial \lambda_1}, \tag{2}$$

$$\sigma_2 + \varepsilon E^2 = \lambda_2 \frac{\partial W_s(\lambda_1, \lambda_2)}{\partial \lambda_2}, \tag{3}$$

where $W_s(\lambda_1, \lambda_2)$ is the Helmholtz free energy associated with stretching the elastomer. The elasticity of the elastomer is balanced by the applied stresses σ_1 and σ_2 , along with the electrostatic interaction—the Maxwell stress εE^2. Equations (1)–(3) constitute the equations of state of an ideal dielectric elastomer.

As mentioned before, after the pull-in instability, the membrane is stabilized by the steep strain-stiffening of the elastomer. Each individual polymer chain in the elastomer has a finite contour length. When the elastomer is subject to no loads, the polymer chains are coiled, allowing a large number of conformations. Subject to loads, the polymer chains become less coiled. As the loads increase, the end-to-end distance of each polymer chain approaches the finite contour length, and the elastomer approaches a limiting stretch. On approaching the limiting stretch, the elastomer stiffens steeply. To account for this behavior, we adopt the Gent model [34]

$$W_s(\lambda_1, \lambda_2) = -\frac{\mu}{2} J_{\lim} \lg\left(1 - \frac{\lambda_1^2 + \lambda_2^2 + \lambda_1^{-2}\lambda_2^{-2} - 3}{J_{\lim}}\right), \tag{4}$$

where μ is the shear modulus, and $J_{\lim}$ is a material constant related to the limiting stretch. When the stretches are small, $\lambda_1^2+\lambda_2^2+\lambda_1^{-2}\lambda_2^{-2}-3 << J_{\lim}$, the Gent model recovers the neo-Hookean model, $W_s(\lambda_1, \lambda_2) = \mu(\lambda_1^2 + \lambda_2^2 + \lambda_1^{-2}\lambda_2^{-2} - 3)/2$. When the stretches approach the limit, $\lambda_1^2+\lambda_2^2+\lambda_1^{-2}\lambda_2^{-2}-3 \to J_{\lim}$, the Gent model stiffens steeply.

A combination of Eqs. (2)–(4) gives the stress-stretch relations

$$\sigma_1 + \varepsilon E^2 = \frac{\mu(\lambda_1^2 - \lambda_1^{-2}\lambda_2^{-2})}{1 - (\lambda_1^2 + \lambda_2^2 + \lambda_1^{-2}\lambda_2^{-2} - 3)/J_{\lim}}, \tag{5}$$

$$\sigma_2 + \varepsilon E^2 = \frac{\mu(\lambda_2^2 - \lambda_1^{-2}\lambda_2^{-2})}{1 - (\lambda_1^2 + \lambda_2^2 + \lambda_1^{-2}\lambda_2^{-2} - 3)/J_{\lim}}. \tag{6}$$

Throughout the paper, we consider an acrylic elastomer VHB4910 (by 3M) with the following representative material parameters: $\varepsilon = 3.98 \times 10^{-11}$ F/m, $\mu = 45$ kPa, $J_{\lim} = 120$ [22, 35]. The density of VHB is ρ =980 kg/m^3 (3M Company).

The membrane is susceptible to various modes of failure. Here we consider two significant modes of failure: electrical breakdown and mechanical rupture. We adopt a constant value of electrical breakdown field $E_{EB} = 200$ MV/m [36, 37]. We assume a simple criterion for rupture: $(\lambda_1^2 + \lambda_2^2 + \lambda_1^{-2}\lambda_2^{-2} - 3)/J_{\lim} = 0.9$.

3 Homogeneous expansion of dielectric elastomer tube

We next apply the model of ideal dielectric elastomers to the homogeneous expansion of a tubular balloon (Fig. 3). In the reference state, the balloon is undeformed and uncharged, and is of thickness H, radius R and length L. The outer and inner surfaces of the balloon are coated with compliant electrodes. In an actuated state, subject to an internal pressure p and a voltage Φ through the thickness, the balloon is of thickness h, radius r and length l, while charges $+Q$ and $-Q$ are spread over the outer and the inner electrodes. The membrane is incompressible, so that $RHL = rhl$. The longitudinal stretch is $\lambda_1 = l/L$, the hoop stretch is $\lambda_2 = r/R$, and the volume enclosed by the balloon is $v = \pi r^2 l$. The balance of forces gives the longitudinal stress $\sigma_1 = pr/(2h)$ and the hoop stress $\sigma_2 = pr/h$. The electric field is $E = \Phi/h = \lambda_1\lambda_2\Phi/H$, and the magnitude of charge on either electrode is $Q = 2\pi rlD$, or

$$Q = 2\pi\varepsilon(\lambda_1\lambda_2)^2 \frac{RL}{H}\Phi. \tag{7}$$

The factor before the voltage defines the capacitance of the balloon, $C = 2\pi\varepsilon(\lambda_1\lambda_2)^2 RL/H$. As remarked in the introduction, the capacitance of the membrane is quadratic in its area, can change enormously when the balloon expands.

Rewrite Eqs. (5) and (6) in a dimensionless form, we obtain that

$$\frac{pR}{2\mu H} = \frac{(\lambda_2^2 - \lambda_1^2)\lambda_1^{-1}\lambda_2^{-2}}{1 - (\lambda_1^2 + \lambda_2^2 + \lambda_1^{-2}\lambda_2^{-2} - 3)/J_{\lim}}, \tag{8}$$

$$\frac{\varepsilon}{\mu}\left(\frac{\Phi}{H}\right)^2 = \frac{(2\lambda_1^2 - \lambda_2^2 - \lambda_1^{-2}\lambda_2^{-2})\lambda_1^{-2}\lambda_2^{-2}}{1 - (\lambda_1^2 + \lambda_2^2 + \lambda_1^{-2}\lambda_2^{-2} - 3)/J_{\lim}}. \tag{9}$$

Once the loading parameters p and Φ are prescribed, Eqs. (8) and (9) determine the stretches λ_1 and λ_2. These equations are nonlinear and, for given values of p and Φ, have multiple solutions (Fig. 3). Take one curve in Fig. 3c as an example. Imagine an experiment in which the pressure is kept constant at $pR/(2\mu H) = 0.1$ and the voltage is ramped up. When the voltage is small, the balloon expands gradually as the voltage increases. When the voltage reaches the peak of the voltage-stretch curve, no state of equilibrium exists nearby with a higher voltage, but the voltage is ramped up by the external mechanism that applied the voltage. Consequently, the balloon expands suddenly, undergoing snap-through instability, and reaches a budged state. As the voltage is ramped up further, the bulged balloon expands continuously.

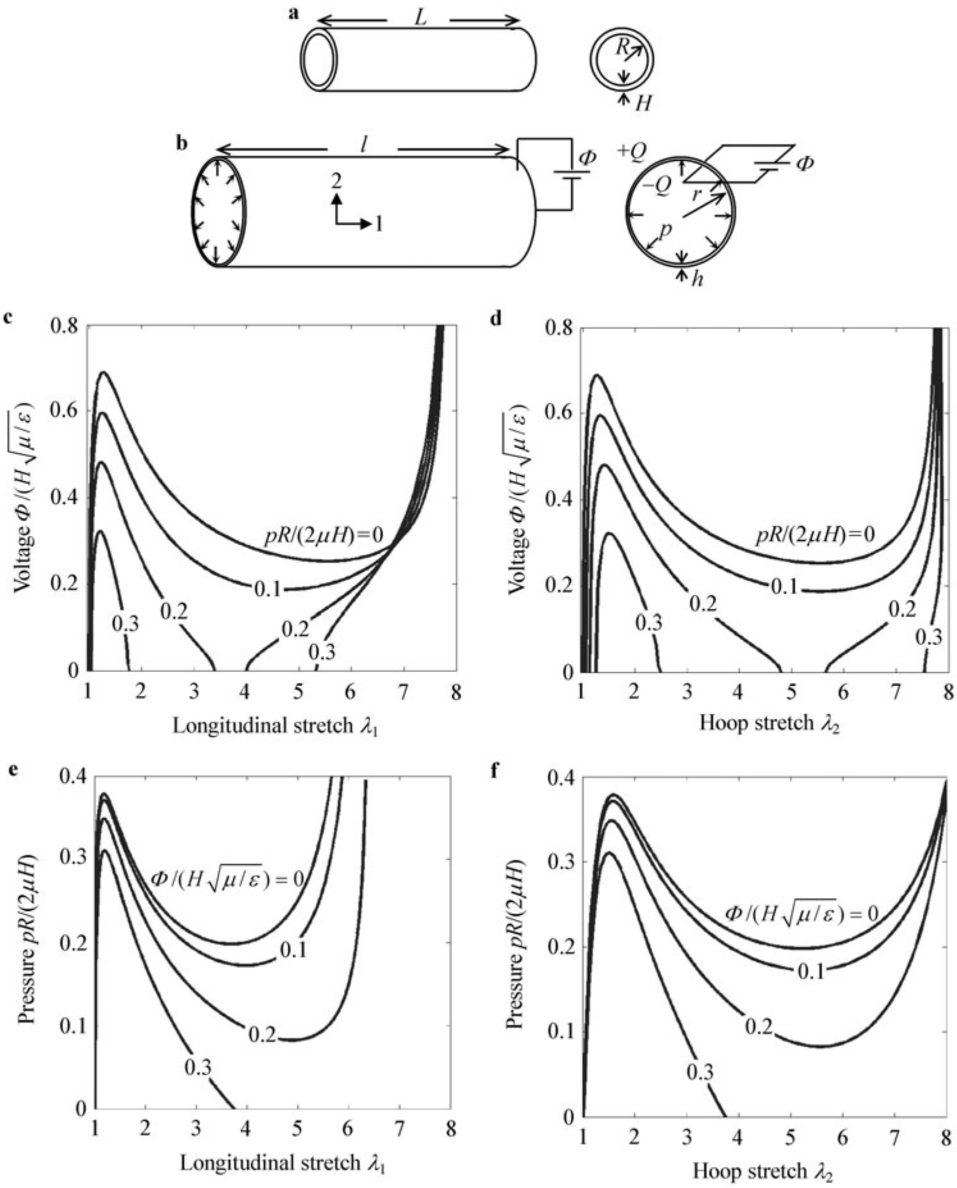

Fig. 3 Homogeneous states of a dielectric elastomer tube subject to internal pressure and voltage. **a** The reference state. **b** An actuated state. **c–f** Various diagrams are used to represent homogeneous states of the balloon

When the pressure is kept constant at $pR/(2\mu H) = 0.2$, the voltage-stretch curve is broken into two parts. The deformation is independent of the sign of the voltage, and only the positive voltage is plotted here.

4 Formation of bulges as an electromechanical phase transition

A bulged and an unbulged section can equilibrate in a balloon (Fig. 4). We now formulate the condition of coexistence following a similar approach described before [25, 26, 28]. In the reference state, the bulged and the unbulged sections are of lengths L' and L'', respectively. In an actuated state, the two sections are of lengths l' and l'', volumes v' and v'', charges Q' and Q'', electric displacements D' and D'', and stretches (λ_1', λ_2') and $(\lambda_1'', \lambda_2'')$. The balloon, along with the mechanisms that apply the voltage and pressure, forms a composite thermodynamic system. The composite is assumed to exchange energy with the rest of the world by heat, but the temperature is held constant. Under the isothermal condition, the composite reaches a state of equilibrium when the Helmholtz free energy of the composite is stationary. The Helmholtz free energy of the composite is the sum of the Helmholtz free energy of the balloon, the potential energy of the mechanisms that apply voltage and pressure. The Helmholtz free energy of the balloon consists of both the elastic energy due to stretching and the dielectric energy: $2\pi RHL'(W_s(\lambda_1', \lambda_2') + (D')^2/(2\varepsilon)) + 2\pi RHL''(W_s(\lambda_1'', \lambda_2'') + (D'')^2/(2\varepsilon))$. The potential energy of the mechanism that applies the voltage is $-\Phi(Q' + Q'')$. The potential energy of the mechanism that applies the pressure is $-p(v' + v'')$. The sum of these contributions gives the Helmholtz free energy of the composite

$$\begin{aligned}\Pi = {} & 2\pi RHL'(W_s(\lambda_1', \lambda_2') + (D')^2/(2\varepsilon)) \\ & -\pi R^2 L'(\lambda_2')^2 \lambda_1' p - 2\pi RL'\lambda_1'\lambda_2' D'\Phi \\ & +2\pi RHL''(W_s(\lambda_1'', \lambda_2'') + (D'')^2/(2\varepsilon)) \\ & -\pi R^2 L''(\lambda_2'')^2 \lambda_1'' p - 2\pi RL''\lambda_1''\lambda_2'' D''\Phi. \end{aligned} \tag{10}$$

Recall that $L' + L'' = L$. When the pressure and voltage are held constant, the Helmholtz free energy of the composite is a function of seven independent variables, $\Pi(D', \lambda_1', \lambda_2', D'', \lambda_1'', \lambda_2'', L')$.

The free-energy function is stationary when the composite reaches a state of equilibrium. Setting the partial derivatives with respect to the independent variables to zero, we obtain seven equations of equilibrium, six of which recover the equations of state (1)–(3) in the bulged and the unbulged sections. The seventh equation, resulting from $\partial\Pi/\partial L' = 0$, is

$$\begin{aligned} & W_s(\lambda_1', \lambda_2') - \frac{pR}{2H}(\lambda_2')^2\lambda_1' - \frac{\varepsilon}{2}\left(\frac{\Phi}{H}\right)^2(\lambda_1'\lambda_2')^2 \\ & = W_s(\lambda_1'', \lambda_2'') - \frac{pR}{2H}(\lambda_2'')^2\lambda_1'' - \frac{\varepsilon}{2}\left(\frac{\Phi}{H}\right)^2(\lambda_1''\lambda_2'')^2. \end{aligned} \tag{11}$$

This equation is the condition for the bulged and unbulged sections to equilibrate in the balloon. The condition is readily understood as follows. Assume that both the bulged and unbulged sections are long compared to the diameter of the

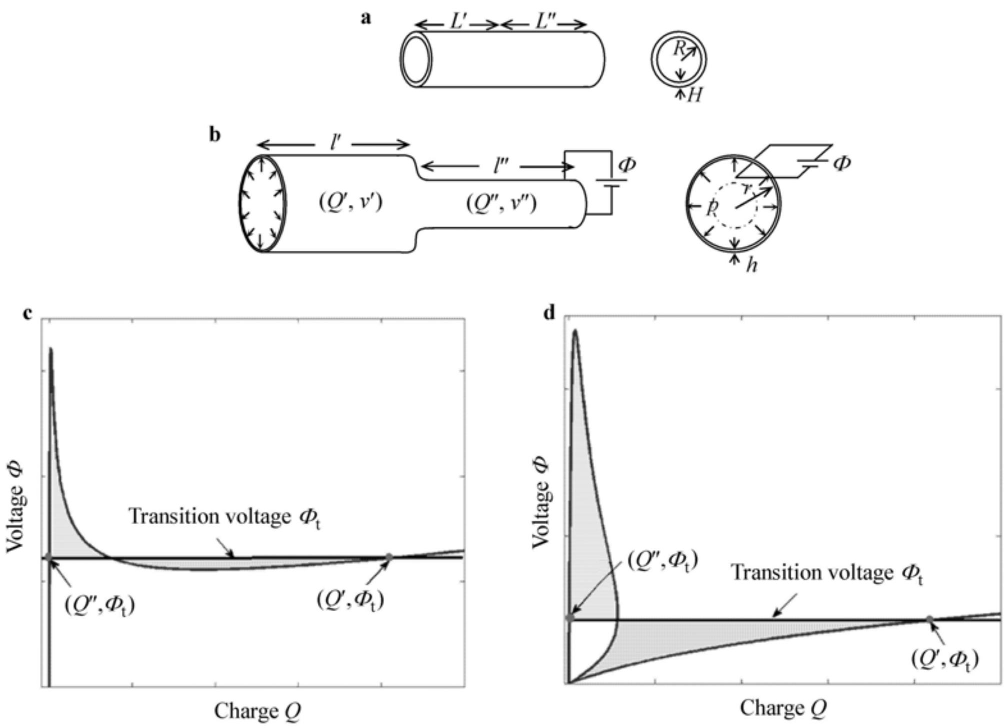

Fig. 4 A bulged section and an unbulged section coexist in a balloon subject to an internal pressure and a voltage through the thickness. **a** In the reference state, the lengths of the bulged and unbulged sections are marked as L' and L''. **b** In an actuated state, the two sections are of lengths l' and l''. **c** At one value of constant pressure, the voltage-charge curve goes up, down, and up again. The bulged and the unbulged sections coexist at the transition voltage Φ_t that makes the two shaded areas equal. **d** At a higher value of constant pressure, the voltage-charge curve starts from the origin, goes up, loops back to the origin, and then goes up again. The bulged and the unbulged sections coexist at the transition voltage Φ_t that makes the two shaded areas equal

balloon. We can speak of the Helmholtz free energy of the composite per unit length of the tube. When the bulged and unbulged sections equilibrate, the Helmholtz free energy of the composite per unit length must equal for the bulged and unbulged sections. Equation (11) can also be represented graphically by using the Maxwell rule [38]. Under a small constant pressure, the voltage-stretch curve goes up, down, and then up again (Fig. 3c). The bulged and the unbulged sections coexist at the transition voltage Φ_t that makes the two shaded areas equal in voltage-charge plane (Fig. 4c). The transition voltage can be much lower than the peak voltage. Under a large constant pressure, the voltage-stretch curve is broken into two parts. In the voltage-charge plane, the curve goes up, loops back to the origin, and then goes up again (Fig. 4d). The transition voltage makes the shaded areas equal.

Given a voltage Φ and a pressure p, the bulged section should be in a state of equilibrium, and the unbulged section should be in another state of equilibrium. Both states satisfy Eqs. (8) and (9). When the two sections equilibrate with each other, Eq. (11) holds. Consequently, the condition of coexistence can be represented by a curve on the voltage-pressure diagram (Fig. 5). Each point in the diagram represents a given pair of voltage and pressure. Below the curve, the entire balloon is unbulged. Above the curve, the entire balloon is bulged. The transition curve intersects with the p-axis, indicating that pressure alone can induce the bulging transition, as is well known. The transition curve also intersects with the Φ-axis, indicating that the voltage alone can induce the transition. This prediction, however, has never been observed experimentally. As will become clear, the bulged state for a balloon without internal pressure suffers electrical breakdown.

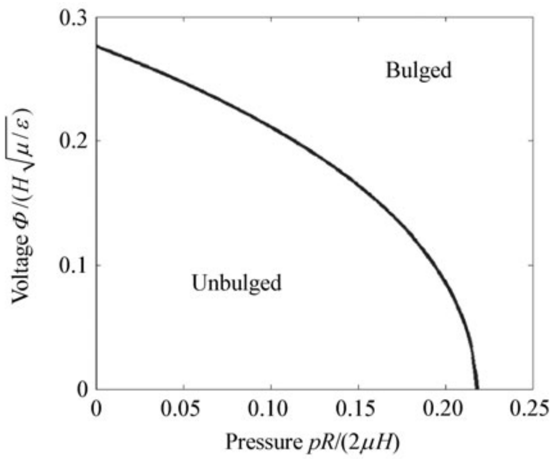

Fig. 5 A bulged and an unbulged section coexist when the values of the pressure and voltage fall on the curve in the pressure-voltage plane. Below the curve, the entire balloon is unbulged. Above the curve, the entire balloon is bulged

The description of a steam engine or a refrigerator has long been aided by diagrams of various independent variables [27]. The description of a electromechanical transducer can be similarly aided [33]. Here we describe a tubular balloon with two degrees of freedom—that is, each state of the balloon is specified by values of two independent variables. For example, one choice of the independent variables can be the voltage and the charge (Fig. 6). Each point in the voltage-charge diagram represents a state of the balloon. The plane can be divided into several regions. The left region corresponds to the states in which the entire balloon is unbulged. The right region corresponds to the states in which the entire balloon is bulged. The middle region corresponds to states in which bulged and unbulged sections coexist in the balloon.

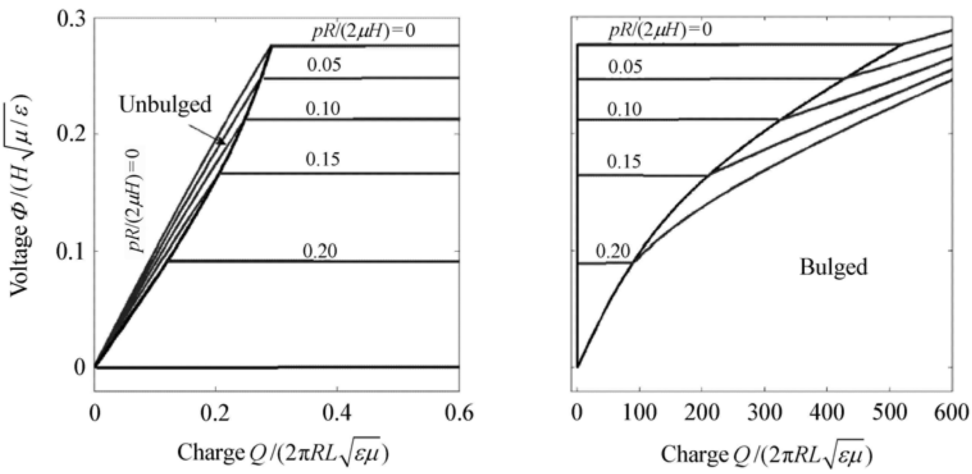

Fig. 6 Constant-pressure curves in the voltage-charge plane. The left figure expands the interval (0, 0.6) of the horizontal axis. When the values of the voltage and charge fall in the region to the left, the entire balloon is unbulged. When the values of the voltage and charge fall in the region to the right, the entire balloon is bulged. A point on a horizontal line corresponds to a balloon with a mixture of bulged and unbulged sections

A curve in the plane represents a sequence of states that constitute a process. As an example, consider a balloon under a constant pressure $pR/(2\mu H) = 0.1$ and a ramp voltage. The slope of the voltage-charge curve defines the capacitance. The capacitance is small when the entire balloon is unbulged, and the capacitance is large when the entire balloon is bulged. In the region of bulging transition, the constant-pressure curve is horizontal. A point on the horizontal line corresponds to a balloon with a mixture of bulged and unbulged sections. For a balloon with a fixed total charge Q, the lengths of the two sections are determined by $Q = (Q'L' + Q''L'')/L$ and $L = L' + L''$, where Q' and Q'' can be read from the two end points of the horizontal line. The state of the balloon of coexistent bulged and unbulged sections can also be described by two parameters, for instance by the total charge Q and the fraction of the bulged section L'/L. The fraction L'/L is analogous to the fraction of the mass of the vapor in a saturated liquid-vapor mixture, a number known as the quality of the mixture.

5 Allowable states, electromechanical cycles, and energy converted per cycle

Not all states of the balloon are allowable. Following an approach described before [39, 40], we represent the allowable states on the plane of work-conjugating variables, such as the voltage-charge diagram and the pressure-volume diagram. The two conditions of failure—breakdown and rupture—are plotted on the voltage-charge diagram (Fig. 7). The conditions of failure, together with conditions $p = 0$ and $\Phi = 0$, define the region of allowable states. We further divide the region of allowable states into three subregions: in subregion I the entire balloon is unbulged, in subregion II the balloon consists of coexistent bulged and unbulged sections, and in subregion III the entire balloon is bulged.

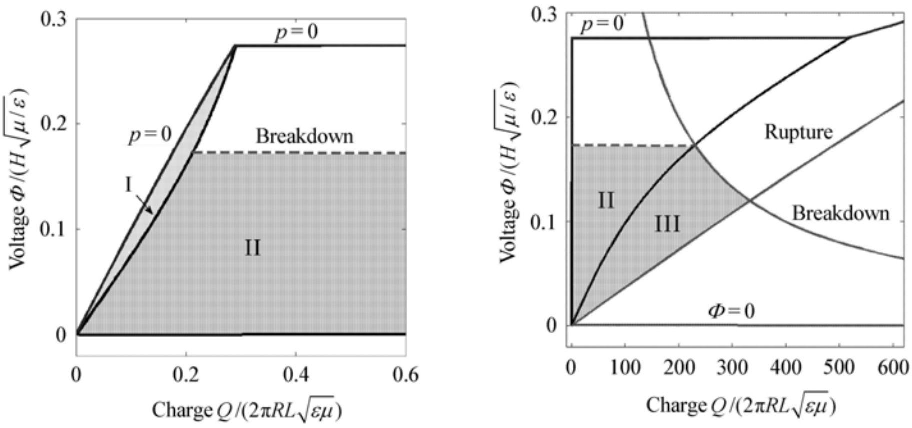

Fig. 7 A region of allowable states is identified on the voltage-charge diagram. The left figure expands the interval (0, 0.6) of the horizontal axis. The curves correspond to the boundary of coexistence, the conditions of electrical breakdown, and the conditions of mechanical rupture. These lines, together with the conditions $p = 0$ and $\Phi = 0$, surround the region of allowable states. The region of allowable states is further divided into three subregions: the entire balloon is unbulged in subregion I, the balloon consists of coexistent bulged and unbulged sections in subregion II, and the entire balloon is bulged in subregion III

When the bulged and the unbulged sections coexist, the former has the higher electric field. Consequently, in the region of the voltage-charge diagram where bulged and unbulged sections coexist, the allowable states are below the dashed line (Fig. 7). The special case $p = 0$ corresponds to a tube subject to no pressure but subject to voltage. The case is the same as a flat membrane considered previously [28, 37]. Under $p = 0$, when the applied voltage is below the transition voltage, the balloon is entirely unbulged. Upon reaching the transition voltage, a small part of the balloon starts to bulge, but before the bulge fully forms the balloon suffers electrical breakdown. By contrast, when the pressure in the tube is high enough, the transition voltage is lowered, so that the balloon forms a bulge without electrical breakdown.

A closed curve in the voltage-charge diagram represents an electromechanical cycle. If the cycle is clockwise, the mechanism of applying the voltage does net work in the cycle, and the balloon acts as an actuator. If the cycle is counterclockwise, the work is done on the mechanism of applying the voltage, and the balloon acts as a generator. In both cases, the amount of work is the area enclosed by the curve. The maximum electromechanical energy converted is achieved by a cycle going along the boundary of the region of the allowable states. The energy density calculated from the area of the region of allowable states is approximately 1.2 J/g. The contributions from the three subregions are 0.02%, 47.29%, 52.69%, respectively.

The area of subregion II is more than 2 000 times that of subregion I. If the cycle only operates in subregion I, the energy converted per cycle is extremely small. The situation is analogous to a practice noted by Carnot: engines do not operate by cycles consisting of only liquid states [41]. In liquid states, the fluid is nearly incompressible and a cycle of liquid states coverts an extremely small amount of energy compared to a cycle of mixed states of liquid and gas. A thermodynamic vapor cycle is analogous to an electromechanical cycle going through a sequence of states in all three subregions, including states of entirely unbulged balloon, states of coexistent unbulged and bulged sections, and states of entirely bulged balloon. A thermodynamic gas cycle is analogous to an electromechanical cycle restricted in subregion III, in which the balloon is bulged in all states of the cycle.

The states of balloon can also be represented on planes of other independent variables. In particular, the pressure and the volume are also work-conjugating variables, so that the pressure-volume diagram is just as effective to describe energy converted in electromechanical cycles (Fig. 8). If a cycle in the pressure-volume diagram is clockwise, the mechanism of applying the pressure does net work in the cycle, and the balloon acts as a generator. If the cycle is counterclockwise, the work is done on the mechanism of applying the pressure, and the balloon acts as an actuator. In both cases, the amount of work is the area enclosed by the curve. Because we have excluded dissipative processes, after a generation cycle is completed, the free-energy recovers its value, and the mechanical work done by the mechanism that applies the pressure equals the electrical work done to the mechanism that applies the voltage. The region of allowable states in the pressure-volume diagram has the same area as that in the voltage-charge diagram.

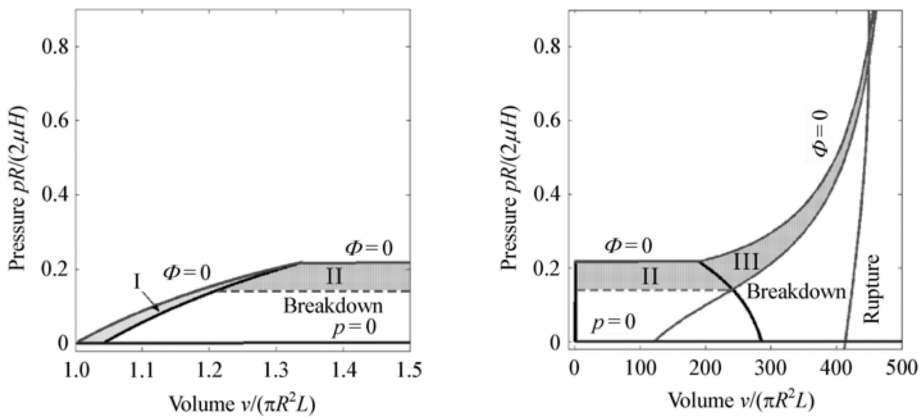

Fig. 8 A region of allowable states is identified on the pressure-volume diagram. The left figure expands the interval (1.0, 1.5) of the horizontal axis. The entire balloon is unbulged in subregion I, the balloon consists of coexistent bulged and unbulged sections in subregion II, and the entire balloon is bulged in subregion III

6 Concluding remarks

The electromechanical phase transition is studied for a propagating bulge in a tubular balloon. The presence of internal pressure reduces the voltage needed for the transition, so that the balloon can form a bulge without electrical breakdown. The bulging transition is analogs to liquid-vapor phase transition. A dielectric elastomer generator cycling through bulged and unbulged states is analogous to a steam engine cycling through liquid and gas states. Energy converted in an electromechanical cycle consisting of unbulged and bulged states is thousands of times that in an electromechanical cycle consisting of only unbulged states. It is hoped that experiments will soon succeed in demonstrating dielectric elastomer generators that convert large amount of energy per cycle by the electromechanical phase transition.

Acknowledgements The project was supported by ARO (W911NF-09-1-0476), DARPA (W911NF-10-1-0113), and MRSEC. Lu is supported by China Scholarship Council as a visiting scholar for two years at Harvard University. Suo acknowledges the Alexander von Humboldt Foundation for the Humboldt Award, and thanks Professor Oliver Kraft, of the Karlsruhe Institute of Technology, for being a gracious host.

References

1 Carpi, F., Bauer, S., De Rossi, D.: Stretching dielectric elastomer performance. Science **330**, 1759–1791 (2010)
2 Brochu, P., Pei, Q.B.: Advances in dielectric elastomers for actuators and artificial muscles. Macromol Rapid Commun. **31**, 10–36 (2010)
3 Shankar, R., Ghosh, T.K., Spontak, R.J.: Electroactive nanostructured polymers as tunable actuators. Adv. Mater. **19**, 2218–2223 (2007)
4 O'Brien, B.M., McKay, T.G., Gisby, T.A., et al.: Rotating turkeys and self-commutating artificial muscle motors. Appl. Phys. Lett. **100**, 074108 (2012)
5 Pei, Q.B., Pelrine, R., Stanford, S., et al.: Electroelastomer rolls and their application for biomimetic walking robots. Syn. Metals **135–136**, 129–131 (2003)
6 Kovacs, G., Düring, L., Michel, S., et al.: Stacked dielectric

elastomer actuator for tensile force transmission. Sens. Actuators A **155**, 299–307 (2009)

7 Carpi, F., Frediani, G., Turco, S., et al.: Bioinspired tunable lens with muscle–like electroactive elastomers. Adv. Func. Mater. **21**, 4152–4158 (2011)

8 Akbari, S., Shea, H.R.: Microfabrication and characterization of an array of dielectric elastomer actuators generating uniaxial strain to stretch individual cells. J. Micromech. Microeng. **22**, 045020 (2012)

9 Cheng, A.: Latest EAP driven commercial product. WW–EAP Newsletter **13**, 2 (2011)

10 McKay, T., O'Brien, B.M., Calius, E., et al.: An integrated, self–priming dielectric elastomer generator. Appl. Phys. Lett. **97**, 062911 (2010)

11 Kaltseis, R., Keplinger, C., Baumgartner, R., et al.: Method for measuring energy generation and efficiency of dielectric elastomer generators. Appl. Phys. Lett. **99**, 162904 (2011)

12 Kornbluh, R.D., Pelrine, R., Prahlad, H., et al.: Dielectric elastomers: Stretching the capabilities of energy harvesting. MRS Bulletin **37**, 246–253 (2012).

13 Stark, K.H., Garton, C.G.: Electric strength of irradiated polythene. Nature **176**, 1225–1226 (1955)

14 Pelrine, R.E., Kornbluh, R.D., Joseph, J.P.: Electrostriction of polymer dielectrics with compliant electrodes as a means of actuation. Sens. Actuators A **64**, 77–85 (1998)

15 Wissler, M., Mazza, E.: Modeling of a pre–strained circular actuator made of dielectric elastomers. Sens. Actuators A **120**, 184–192 (2005)

16 Mockensturm, E.M., Goulbourne, N.: Dynamic response of dielectric elastomers. Int. J. Non-linear Mech. **41**, 388–395 (2006)

17 Zhao, X.H., Suo, Z.G.: Method to analyze electromechanical stability of dielectric elastomers. Appl. Phys. Lett. **91**, 061921 (2007)

18 Zhao, X.H., Suo, Z.G.: Theory of dielectric elastomers capable of giant deformation of actuation. Phys. Rev. Lett. **104**, 178302 (2010)

19 Koh, S.J.A., Li, T.F., Zhou, J.X., et al.: Mechanisms of large actuation strain in dielectric elastomers. J. Poly. Sci. B **49**, 504–515 (2011)

20 Pelrine, R., Kornbluh, R., Pei, Q.B., et al.: High-speed electrically actuated elastomers with strain greater than 100%. Science **287**, 836–839 (2000)

21 Kollosche, M., Zhu, J., Suo, Z.G., et al.: Complex interplay of nonlinear processes in dielectric elastomers. Phys. Rev. E **85**, 051801 (2012)

22 Huang, J. S., Li, T.F., Foo, C. C., et al.: Giant, voltage-actuated deformation of a dielectric elastomer under dead load. Appl. Phys. Lett. **100**, 041911 (2012)

23 Keplinger, C., Li, T.F., Baumgartner, R., et al.: Harnessing electromechanical instabilities in dielectric elastomers to achieve giant deformation of actuation. Soft Matter. **8**, 285–288 (2012)

24 Plante, J.S., Dubowsky, S.: Large–scale failure modes of dielectric elastomer actuators. Int. J. Solids Struct. **43**, 7727–7751 (2006)

25 Zhao, X.H., Hong, W., Suo, Z.G.: Electromechanical hysteresis and coexistent states in dielectric elastomers. Phys. Rev. B **76**, 134113 (2007)

26 Zhou, J.X., Hong, W., Zhao, X.H., et al.: Propagation of instability in dielectric elastomers. Int. J. Solids Struct. **45**, 3739–3750 (2008)

27 Borgnakke, C., Sonntag, R.E.: Fundamentals of Thermodynamics. (7th edn). John Wiley & Sons, Inc. (2008)

28 Huang, R., Suo, Z.G.: Electromechanical phase transition in dielectric elastomers. Proc. Royal. Soci. A **468**, 1014–1040 (2011)

29 Levine, S., Ouchi, M.: The Ultimate Balloon Book. Sterling Publishing Co., Inc. New York (2001)

30 Mallock, A.: Note on the instability of India–rubber tubes and balloons when distended by fluid pressure. Proc. Roy. Soc. London **49**, 458–463 (1891)

31 Chater, E., Hutchinson, J.W.: On the propagation of bulges and buckles. J. Appl. Mech. **51**, 269–277 (1984)

32 Gent, A.N.: Elastic instabilities of inflated rubber shells. Rubber. Chem. Technol. **72**, 263–268 (1999)

33 Suo, Z.G.: Theory of dielectric elastomers. Acta Mech Solida Sinica **23**, 549–578 (2010)

34 Gent, A.N.: A new constitutive relation for rubber. Rubber Chem. Technol. **69**, 59–61 (1996)

35 Kofod, G.: The static actuation of dielectric elastomer how does pre–stretch improve actuation. J. Phys. D Appl. Phys. **41**, 215405 (2008)

36 Kofod, G., Kornbluh, R., Pelrine, R., et al.: Actuation response of polyacrylate dielectric elastomers. J. Intel. Mater. Sys. Struct. **14**, 787–793 (2003)

37 Lu, T.Q., Huang, J.S., Jordi, C., et al.: Dielectric elastomer actuators under equal–biaxial forces, uniaxial forces, and uniaxial constraint of stiff fibers. Soft Matter. **8**, 6167–6173 (2012)

38 Maxwell, J.C.: Theory of Heat. Longmans, Green, and Co. (1872)

39 Koh, S.J.A., Keplinger, C., Li, T.F., et al.: Dielectric elastomer generators: how much energy can be converted. IEEE/ASME Trans. Mechatron. **16**, 33–41 (2011)

40 Koh, S.J.A., Zhao, X.H., Suo, Z.G.: Maximal energy that can be converted by a dielectric elastomer generator. Appl. Phys. Lett. **94**, 262902 (2009)

41 Carnot, S.: Reflections on the Motive Powers of Heat (1824). English translation by R.H. Thurston is freely available online at http://archive.org